Planta (2006) 224: 520–532
DOI 10.1007/s00425-006-0240-1

ORIGINAL ARTICLE

Judy A. Schnurr · Kathleen K. Storey
Hans-Joachim G. Jung · David A. Somers
John W. Gronwald

UDP-sugar pyrophosphorylase is essential for pollen development in Arabidopsis

Received: 16 December 2005 / Accepted: 26 January 2006 / Published online: 24 March 2006

Abstract Arabidopsis UDP-sugar pyrophosphorylase (AtUSP) is a broad substrate enzyme that synthesizes nucleotide sugars. The products of the AtUSP reaction can act as precursors for the synthesis of glycolipids, glycoproteins, and cell wall components including pectin and hemicellulose. AtUSP has no close homologs in Arabidopsis and its biological function has not been clearly defined. We identified two T-DNA insertional mutant lines for AtUSP, *usp-1* and *usp-2*. No homozygous individuals were identified and progeny from plants heterozygous for *usp-1* or *usp-2* showed a 1:1 segregation ratio under selection. Despite decreased levels of both *AtUSP* transcript and USP activity (UDP-GlcA → GlcA-1-P), heterozygous plants were indistinguishable from wild type at all stages of development. Reciprocal test crosses indicated the source of the segregation distortion was lack of transmission through the male gametophyte. Analysis of pollen tetrads from *usp-1* in the *quartet* background revealed a 2:2 ratio of normal:collapsed pollen grains. The collapsed pollen grains were not viable as determined by Alexander's viability and DAPI staining, and pollen germination tests. The pollen phenotype of *usp-1* was complemented by transformation of *usp-1* with the *AtUSP* cDNA sequence. Surface and ultrastructural analyses of pollen from wild-type and *usp* mutants demonstrated that the mutation had no apparent effect on the outer wall (exine) but prevented the synthesis of the pectocellulosic inner wall (intine). Evidence presented here shows that AtUSP has a critical role in pollen development.

Keywords Arabidopsis · Intine · Pollen · *Quartet* · UDP-sugar pyrophosphorylase · USP

Abbreviations Ara: arabinose · Fuc: fucose · Gal: galactose · Glc: glucose · GlcA: glucuronic acid · Man: mannose · GlcNAc: N-acetylglucosamine · Rha: rhamnose · UDP: uridine diphosphate · Xyl: xylose · *NPTII*: neomycin phosphotransferase II

J. A. Schnurr · H.-J. G. Jung · J. W. Gronwald (✉)
USDA-ARS, Plant Science Research,
St. Paul, Minnesota, 55108, USA
E-mail: gronw001@umn.edu
Tel.: +1-612-6258186
Fax: +1-651-6495058

K. K. Storey · D. A. Somers
Department of Agronomy & Plant Genetics,
University of Minnesota, St. Paul, Minnesota 55108, USA

Present address: D. A. Somers
Monsanto Company, Agracetus Campus,
Middleton, WI 53562, USA

Introduction

UDP-sugar pyrophosphorylase (USP), recently cloned and characterized in pea (*Pisum sativum* L), is a broad substrate pyrophosphorylase (Kotake et al. 2004). The enzyme from pea (PsUSP) exhibited high activity with Glc-1-P, Gal-1-P, GlcA-1-P and Ara-1-P, but low activity with GlcNAc-1-P, Fuc-1-P and Glc-6-P. Kotake et al. (2004) proposed that PsUSP functions in the salvage pathway for the synthesis of nucleotide sugars. In this pathway, sugars released from polysaccharides and glycoconjugates by hydrolysis are phosphorylated by C-1 kinases and then converted to UDP-sugars by the subsequent action of a pyrophosphorylase (Feingold and Avigad 1980). In this capacity, USP would play a key role in the turnover and recycling of sugars, such as Ara and Gal, during cell wall synthesis and modification (Gibeaut and Carpita 1991; Lozovaya et al. 1996; Gorshkova et al. 1997).

The USP homolog from Arabidopsis was recently cloned and characterized (L.A. Litterer et al., submitted). Arabidopsis appears to contain a single *USP* gene, as no obvious homologs are present in the genome. AtUSP is similar to PsUSP in that it exhibited high activity with Glc-1-P, Gal-1-P and GlcA-1-P. However,

there were differences between PsUSP and AtUSP. AtUSP had a pH optimum in the range of 7.5–8.5 which is similar to other plant pyrophosphorylases (Otozai et al. 1973; Sowokinos et al. 1993). In contrast, PsUSP had a pH optimum in the range of 6.5–7.5 (Kotake et al. 2004). Furthermore, AtUSP had a three-fold lower K_m for GlcA-1-P compared to PsUSP.

Based on high activity and affinity for GlcA-1-P, it was proposed that AtUSP may function as the terminal enzyme of the *myo*-inositol oxidation (MIO) pathway (L.A. Litterer et al., submitted). The terminal enzyme of the MIO pathway is UDP-GlcA pyrophosphorylase (EC 2.7.7.44) which catalyzes the conversion of GlcA-1-P to UDP-GlcA (Feingold and Avigad 1980). UDP-GlcA pyrophosphorylase activity has only been characterized in semi-purified fractions (Feingold et al. 1958; Roberts 1971; Roberts and Cetorelli 1973; Dickinson et al. 1977; Feingold and Avigad 1980; Hondo et al. 1983) and the gene has not been identified. The MIO pathway is one of two pathways responsible for the synthesis of UDP-GlcA in plants (Feingold and Avigad 1980; Loewus and Loewus 1983; Kärkönen 2005). The second pathway, the nucleotide sugar oxidation (NSO) pathway, involves the conversion of UDP-Glc to UDP-GlcA catalyzed by UDP-Glc dehydrogenase (EC 1.1.1.22). In plants, the relative contributions of the two pathways to the formation of UDP-GlcA are not clearly defined but appear to be dependent on tissue and stage of development (Seitz et al. 2000; Kärkönen 2005).

AtUSP is widely expressed in various tissues of Arabidopsis as indicated by enzyme activity (UDP-GlcA as substrate) and transcript abundance as determined by semi-quantitative RT-PCR and in silico profiles from publicly available microarray data (L.A. Litterer et al., submitted). Evaluation of tissue-specific expression using AtUSP*prom*:GUS constructs indicated high expression in the inflorescence, particularly in pollen grains. These results suggested that AtUSP plays a key role in pollen development perhaps due to its proposed functions in the salvage pathway (Kotake et al. 2004) and/or the synthesis of UDP-GlcA via the MIO pathway (L.A. Litterer et al., submitted).

To better define the role of AtUSP in plant metabolism, we identified two mutant lines (*usp-1*, *usp-2*) from the SIGnAL database containing T-DNA insertional events in the *AtUSP* genomic fragment and isolated mutants. In these lines, a deviation from the expected 3:1 segregation ratio was observed. Genetic analysis by reciprocal test crosses indicated that transmission of the mutant *usp* allele was completely blocked in the male gametophyte. Pollen tetrads from heterozygous *usp-1* mutants in the *quartet* (*qrt1*) background contained two normal and two collapsed pollen grains. Microscopic analyses indicated that the mutation had little or no effect on exine formation, but intine was absent in mature pollen. Possible roles of AtUSP in pollen development are discussed.

Materials and methods

Plant material

Arabidopsis seeds were imbibed and stored at 4°C for 3 days before planting. After stratification, seeds were planted on commercial potting mix and grown at 21°C under a 24 h photoperiod. Kanamycin selection was done by plating sterilized seed (20% bleach, 0.1% SDS for 20 min) on MS medium (4.3 g/L MS salts, 1% sucrose, 0.35% Phytagel, pH 5.7) supplemented with kanamycin (75 mg/L) and scored after 10 days. Basta selection was performed by spraying 7–14-days-old seedlings with 25 mg/L glufosinate ammonium (Liberty 200SL, Bayer CropScience, USA). Three treatments were applied over a 1 week period before plants were scored. To examine gametophytic transmission of the *usp-1* allele, reciprocal test crosses were performed. Resultant seeds were harvested and sown on potting mix for treatment with Basta. Mention of trade names or commercial products in this publication is solely for the purpose of providing specific information and does not imply recommendation or endorsement by the U.S. Department of Agriculture.

Isolation of T-DNA knockout lines

Mutant lines containing putative T-DNA insertions in the At5g52560 (*AtUSP*) gene were obtained through http://signal.salk.edu/cgi-bin/tdnaexpress. Seed was obtained from ABRC and plated on MS medium, and germinated seedlings were transferred to commercial potting mix. The *usp-1* allele is from the SAIL population (SAIL_223_B12; Sessions et al. 2002) and the *usp-2* allele is from the SALK population (SALK_015903; Alonso et al. 2003). To simplify cataloging, seed received from the ABRC was designated the T_1 generation. Genomic DNA was isolated according to Klimyuk et al. (1993). To screen for the presence of a wild-type *AtUSP* allele in *usp-1* and *usp-2* lines, two gene-specific primers were used (USP5; 5′-CGGGATCCATGGCTTCTACG GTTGATTC-3′ and USP3; 5′-CGGGATCCTCAATC TTCAACAGAAATTTGCC-3′). The USP3 primer in combination with the left border primer LB1 (5′-GCC TTTTCAGAAATGGATAAATAGCCTTGCTTCC-3′) for *usp-1* and LBa1 (5′-TGGTTCACGTAGTGGGC CATCG-3′) for *usp-2* was used to screen for the presence of a mutant allele. The right border primer used for the SAIL line was qRB1 (5′-CAAACTAGGATAAATTA TCGCGCGCGGTGTC-3′). Genomic DNA was screened with Takara ExTaq (Fisher Scientific, Fairlawn, NJ) using a thermocycler program of 38 cycles: 94°C for 30 s, 57°C for 30 s, and 72°C for 2 min. The mutant lines identified as hemizygous for the T-DNA insertion in the *AtUSP* gene are referred to as heterozygous throughout the manuscript.

Construction of complementation vector and plant transformation

Amplification of DNA fragments for construction of vectors was done using Expand High Fidelity PCR System (Roche Applied Science, Indianapolis, IN). The complementation vector, pJS17, was created by using several plasmids. The *AtUSP* cDNA fragment was amplified by PCR. Primers contained flanking *Bam*HI/*Sst*I restriction sites (cDNABam5: 5′-TGGATCCA TGGCTTCTACGGTTGATTC-3′; cDNASst3: 5′-AG AGCTCTCAATCTTCAACAGAAAATTTG-3′). The *USPprom* fragment (2.0 kb) was amplified from genomic DNA with promSal5 (5′-AGTCGACGTTATCC TTTGAAAGCATTC-3′) and promSal3 (5′-TGTCGAC GAAGAGGCTCTTAACAAAGG-3′) primers. The PCR products were cloned into pGEM-T Easy (Promega, Madison, WI) to create pJS14 and pJS15, respectively. Both pBI101.1 and pJS14 were restricted with *Bam*HI and *Sst*I and appropriate vector/insert bands were gel purified and ligated together. The resultant vector, pJS16, contained a promoterless *AtUSP* cDNA fragment in place of the *GUS* fragment. The *Sal*I-flanked *AtUSPprom* fragment was subcloned into pJS16 to create pJS17. The transformation vector, pJS17, was electroporated into electrocompetent Agrobacterium (GV3101). Basta-resistant *usp-1* plants were transformed according to Clough and Bent (1998). Putatively transformed plants were screened for the presence of the *NPTII* fragment with NPT5 (5′-GCTATGACTGGGC ACAACAGAC-3′) and NPT3 (5′-CGTCAAGAAGGC GATAGAAGG-3′).

Analysis of *AtUSP* transcripts

Northern blot analysis was performed by isolating total RNA from flowers and buds using TRIzol reagent according to manufacturer's instructions (Invitrogen, Carlsbad, CA). Separation, transfer, probe synthesis, and hybridization were done as described previously (Schnurr et al. 2004). The probe template was a full-length *AtUSP* cDNA fragment generated with the USP5 and USP3 primers.

Pollen histology and in vitro germination of pollen

Phenotyping of pollen was done by gently pressing opened flowers onto solidified medium (1.5% agar) and viewing under a light microscope. Histochemical GUS staining was performed according to Jefferson et al. (1987) and included vacuum infiltration of the substrate. Alexander's staining of pollen was done by adding a 1:25 dilution of Alexander's stain in water to a microscope slide containing released pollen grains (Alexander 1969; Johnson-Brousseau and McCormick 2004). Analysis of mature pollen with DAPI was performed by incubation of pollen for 30 min in buffer containing 0.1% Nonidet P40, 10% DMSO, 50 mM PIPES, pH 6.9, 5 mM EGTA, and 5 μg/mL DAPI. Preparations were examined with an inverted light microscope (Olympus IX70, Melville, NY) equipped with fluorescence imaging.

Pollen germination was determined by incubating released pollen with medium containing 17% sucrose, 2 mM $CaCl_2$, 1.65 mM H_3BO_3, and 0.6% agar, pH 7.0. After a 6–15 h incubation at room temperature under illumination, germinating pollen grains were scored using light microscopy.

Scanning and transmission electron microscopy

For SEM, pollen from open flowers was placed on stubs and sputter-coated with gold particles. Specimens were viewed using a Hitachi S-3500 N scope. To analyze ultrastructure, sepals and petals were removed from buds, and dissected buds were vacuum infiltrated with fixative (2.5% glutaraldehyde, 2.5% paraformaldehyde, 0.1 M phosphate buffer pH 6.8, 0.1% Triton X-100) and incubated overnight at 4°C. Buds were rinsed and fixed in 2% OsO_4 in 0.1 M phosphate buffer, pH 6.8 for 1 h. After dehydration through an ethanol series, buds were embedded with Embed812. At each step, a modified microwave procedure was combined with conventional incubation times to ensure infiltration using a Pelco 3441 Laboratory Microwave System (Ted Pella, Inc, Redding, CA; Giberson et al. 1997). Ultrathin sections were stained with uranyl acetate and triple lead stain (Hanaichi et al. 1986) and viewed with a Phillips CM12 TEM. At each stage of anther development, a minimum of three sections from buds off two heterozygous *usp-2* plants were viewed with TEM.

Cell wall analysis

Seed from a heterozygous line (L9HET) was planted on commercial potting mix. After 42 days, the phenotype of pollen tetrads was determined. Plants were harvested by removing inflorescences from rosettes and removing flowers, buds, siliques, and cauline leaves from stems. Samples were dried at 52°C for 3 days. Dried rosette and stem samples were pulverized in a shaking ballmill (Spex CertiPrep 8000; Metuchen, NJ) for subsequent chemical analyses. Stem cell wall concentration and composition were determined on the dried samples using the Uppsala dietary fiber method (Theander et al. 1995). Briefly, after removal of simple sugars and starch using enzymes and 80% ethanol, the cell wall residues were hydrolyzed with sulfuric acid in a two-stage procedure. Klason lignin was measured gravimetrically as the ash-free, nonhydrolyzed residue and the neutral sugar components of the cell wall polysaccharides were determined as alditol-acetate derivatives by gas chromatography. Uronic acid polysaccharide components were measured colorimetrically in an aliquot from the first step of the acid-hydrolysis procedure using galacturonic acid as the calibration

standard (Ahmed and Labavitch 1977). Total cell wall concentration was calculated as the sum of Klason lignin, glucose, xylose, mannose, fucose, uronic acids, arabinose, galactose and rhamnose residues. All data were corrected to an organic matter basis by determining 100°C dry matter content overnight and subsequent ashing at 450°C for 6 h. All analyses were conducted in duplicate. The study was repeated a total of three times and statistically analyzed as a randomized complete block with three replications. Concentrations of all components except Klason lignin were significantly different between rosettes and stems, and no significant line (WT vs. HET) by tissue (rosette vs. stem) interactions were present ($P > 0.05$).

UDP-GlcA pyrophosphorylase assay

Segregating progeny from a heterozygous line (L9HET) were grown on commercial potting mix. Upon flowering, the phenotype of pollen tetrads was determined with light microscopy. Approximately 1 g fresh wt of rosette tissue from wild-type or heterozygous *usp-1* plants was ground in 5 ml extraction buffer [50 mM Tris-Cl (pH 8.0), 1 mM $MgCl_2$, 0.5 M KCl, 0.1% (v/v) Triton X-100, 0.07% (v/v) β-mercaptoethanol, 0.5 mM phenylmethanesulfonyl fluoride] and then filtered through Miracloth. Extracts were centrifuged at 12,000*g* for 10 min at 4°C. After filtering through Miracloth, 2.5 ml of supernatant was loaded onto a PD-10 column (Amersham Pharmacia Biotech, Piscataway, NJ) and eluted with desalting buffer [50 mM Tris-Cl (pH 8.0), 1 mM $MgCl_2$, 10% (v/v) glycerol, 0.07% (v/v) β-mercaptoethanol]. USP activity in the reverse direction was determined by measuring the formation of [^{14}C]GlcA-1-P from UDP-[^{14}C]GlcA and inorganic pyrophosphate using a modification of the protocol described by Szumilo et al. (1996). The reaction mixture contained the following in a final volume of 50 µl: 100 mM TAPS (pH 8.0), 2 mM $MgCl_2$, 2 mM UDP-[^{14}C]GlcA (1.85×10^7 Bq mmol^{-1}), 5 mM sodium pyrophosphate and desalted crude extract (20 µl). After 30 min incubation at 30°C, the reaction was stopped by adding 0.5 ml 5% (w/v) TCA, followed by addition of 0.3 ml ENVI-Carb 120/400 (Sigma-Aldrich, St. Louis, MO) (150 mg ml^{-1} in water). After 2 min of mixing, the mixture was loaded onto a 2 ml, 0.2 µm nylon filter spin unit (Chrom Tech, Inc., AppleValley, MN). After a 1 min spin at 1,000*g*, 0.5 ml was counted in 10 ml EcoLume. Blank controls contained all components except sodium pyrophosphate.

Results

Isolation of *usp* alleles

Two lines with a predicted T-DNA insertion in the *AtUSP* genomic fragment were identified in the SIGnAL database (http://signal.salk.edu/cgi-bin/tdnaexpress). The first, designated *usp-1*, was from the Syngenta collection (SAIL_223_B12; Sessions et al. 2002). The T-DNA used to generate the *usp-1* line contains the *BAR* gene. The second line, *usp-2*, was from the Salk Institute collection (SALK_015903; Alonso et al. 2003). The T-DNA that generated *usp-2* contains the *NPTII* gene for selection.

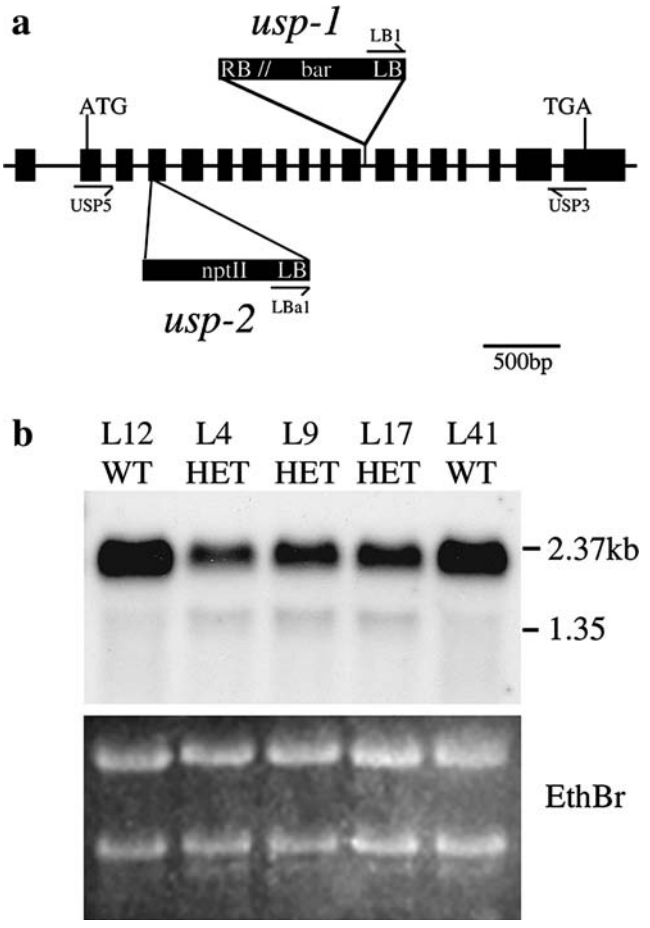

Fig. 1 **a** Diagram of *AtUSP* showing two T-DNA insertional alleles, *usp-1* and *usp-2*. Primers used in PCR screens are included. **b** Northern blot analysis of total RNA isolated from wild-type (L12WT, L41WT) and heterozygous *usp-1* mutants (L4HET, L9HET, L17HET). Ethidium bromide is provided as a loading control

To identify individuals containing T-DNA-interrupted *usp-1* or *usp-2* alleles, genomic DNA isolated from putative *usp* plants was screened by PCR using a gene-specific primer combination or a T-DNA border primer paired with a gene-specific primer. Fig. 1a diagrams the *AtUSP* DNA fragment and indicates the location of primers used in the screen. To detect a wild-type copy of the *AtUSP* gene, primer USP5 was used in combination with primer USP3 (Fig. 1a). The presence of a band generated with the USP3 primer in combination with the left border primer (LB1 or LBa1) indicated the presence of a mutant *usp* allele. In DNA from *usp-1* individuals, the size of the PCR product generated with the mutant allele primer combination is consistent

with the predicted insertion site shown at the SIGnAL database. Sequence analysis of the gel-purified PCR product revealed that the first 171 bases were identical to LB sequence, while the remaining 1.5 kb was identical to *AtUSP* genomic sequence (BACF6N7; gi|4589412). Therefore, the T-DNA insertion occurred 1,812 bp downstream of the *AtUSP* start codon between exons 11 and 12. PCR on the same *usp-1* genomic DNA using the right border primer in combination with USP5 yielded a product of 1.9 kb (data not shown). Subsequent sequencing of this PCR product revealed that 134 bp of right border sequence were followed by sequence with identity to *AtUSP* genomic DNA sequence upstream of the insertion. Further details into the nature of the *usp-1* insertion were not investigated.

Genomic DNA isolated from putative *usp-2* plants was also screened with PCR using both gene-specific and mutant allele primer combinations. The PCR product generated by using the LBa1 primer in combination with USP3 was gel-purified for sequence analysis. Left border sequence (76 bp) was present and the remainder of the PCR product was identical to *AtUSP* genomic sequence. In *usp-2*, the T-DNA is inserted at 394 bp downstream from the *AtUSP* start codon (in exon 4), near the predicted insertion site in the SIGnAL database. Results of PCR analysis of the insertion site from the right border were inconclusive and were not investigated further.

In the screen of *usp-1* and *usp-2* T_1 individuals, we were unable to identify an individual homozygous for either mutant *usp* allele. The T_1 plants were allowed to self and resultant seed was scored for segregation under Basta selection. For *usp-1*, T_2 seed was germinated on potting mix and seedlings were treated with Basta. Two lines that showed 100% sensitivity to Basta and three lines that showed segregation were chosen for further analysis. All of the seedlings tested from lines L12WT and L41WT were sensitive to Basta ($n = 154$, 149, respectively). In T_2 seedlings from lines L4HET (5 of 19 Ba^R), L9HET (8 of 24 Ba^R) and L17HET (7 of 14 Ba^R), Basta resistance ranged from 26 to 50%. Using PCR, genomic DNA was screened with gene-specific primer and mutant allele primer combinations to determine individual plant genotypes at the *AtUSP* locus. DNA from the 20 Basta-resistant plants from the L4HET, L9HET and L17HET lines yielded bands for both wild-type and *usp-1* alleles, indicating they were heterozygous at the *usp-1* locus. Similarly, the T_1 *usp-2* plants were allowed to self and T_2 progeny were plated on medium containing kanamycin. Seedlings of one line, A1WT, were 100% sensitive to kanamycin ($n = 151$). A second line, A8HET, showed a segregation pattern approaching a 1:1 ratio (resistant:sensitive). Of 254 seedlings, 118 were kanamycin-resistant ($\chi^2 = 1.3$; $P > 0.25$). Eighteen Kan^R T_2 seedlings were transferred off plates to potting mix. Genomic DNA was isolated and screened with gene-specific primers and the mutant allele primer combination (Fig. 1a). DNA from all 18 Kan^R individuals yielded bands corresponding to both a wild-type and mutant *usp-2* allele, indicating they were heterozygous at the *usp-2* locus.

To determine if insertion of the T-DNA caused an alteration in the size or abundance of the *AtUSP* transcript, we analyzed RNA expression by Northern blot analysis. Total RNA was isolated from flowers and buds of Basta-resistant *usp-1* individuals of lines L12WT, L41WT, L4HET, L9HET, and L17HET and the results are summarized in Fig. 1b. The size of the hybridizing sequence in RNA from L12WT and L41WT was consistent with the predicted length from published cDNA sequence (2.286 kb; gb|AF360236.1). Bands of the same size are present in RNA from heterozygous, Basta-resistant individuals from lines L4HET, L9HET, and L17HET, but were reduced in abundance (Fig. 1b).

Genetic analysis of *usp* mutants

In *usp-1*, 143 (of 314) seedlings from line L9HET exhibited resistance to Basta, which was a good fit to a 1:1 ratio ($\chi^2 = 2.5$; $P > 0.1$). To determine if the lack of identifiable homozygous mutants in both populations was due to seed mortality or lack of germination, we tested germination of T_2 seed from *usp-1* and *usp-2* heterozygous lines. When *usp-1* seed (T_2) was sterilized, stratified and sown on non-selective medium, line L12WT showed 99% germination ($n = 92$), while 100% of seed from L9HET germinated ($n = 157$). For *usp-2*, seed from both A1WT and A8HET showed 97% germination ($n = 92$ and 106, respectively). On commercial potting mix, lines L12WT and L9HET showed 98 and 100% germination ($n = 100$), while seed from A1WT and A8HET showed 100 and 96% germination, respectively ($n = 100$).

The deviation from the 3:1 segregation ratio could not be explained by lack of seed viability. To determine the cause of segregation distortion, we performed reciprocal test crosses. The genetic background of the *usp-1* mutants is *quartet1* (*qrt1*), which facilitated our gametophytic analysis (Sessions et al. 2002). In the *qrt1* background, all four products of male meioses are held together in a tetrad throughout pollen development (Preuss et al. 1994). Plants heterozygous by PCR analysis (*qrt1*/*qrt1*;*USP*/*usp-1*) were reciprocally crossed with progeny from lines where 100% of individuals tested were sensitive to Basta (*qrt1*/*qrt1*;*USP*/*USP*). As shown in Table 1, progeny from selfed *qrt1*/*qrt1*;*USP*/*USP*

Table 1 Results of reciprocal test crosses with *usp-1* heterozygous and wild-type individuals

Female parent	Male parent	Resistant*	Sensitive*
qrt1/qrt1;USP/USP	Selfed	0	213
qrt1/qrt1;USP/usp-1	Selfed	62	63
qrt1/qrt1;USP/usp-1	*qrt1/qrt1;USP/USP*	101	94
qrt1/qrt1;USP/USP	*qrt1/qrt1;USP/usp-1*	0	174

*Seed from resultant crosses were scored by resistance to Basta

plants showed 100% sensitivity to Basta ($n = 213$). In progeny from selfed *qrt1*/*qrt1*;*USP*/*usp-1* lines, 50% of resultant seedlings were resistant to Basta (Table 1). With *qrt1*/*qrt1*;*USP*/*USP* as the pollen donor on receptive stigmas of *qrt1*/*qrt1*;*USP*/*usp-1*, 52% of resultant seedlings were resistant to Basta, which showed a transmission efficiency (TE) through the female of 100% (calculated according to Howden et al. 1998). In contrast, when *qrt1*/*qrt1*;*USP*/*usp-1* was the pollen donor on *qrt1*/*qrt1*;*USP*/*USP* stigmas, none of the resultant seedlings were Basta-resistant (Table 1). A TE through the male of 0% indicates that the male gamete was the cause of the distortion observed in segregating populations. The total seed set of wild-type and heterozygous *usp-1* plants was not statistically different, further supporting the result that the female gametophyte was not affected (data not shown).

Phenotype of pollen in *usp-1* and *usp-2*

To determine if a visible phenotype was present in pollen from heterozygous mutants, we screened the 20 Basta-resistant *usp-1* T_2 individuals from L4HET, L9HET and L17HET (heterozygous as determined by PCR analysis). Pollen from open flowers was collected on solidified medium and observed using light microscopy. From all 20 lines, pollen tetrads showed the same phenotype. As shown in Fig. 2b, of the four pollen grains of the tetrad, two were visibly shrunken compared to tetrads isolated from wild type (Fig. 2a). Similarly, pollen from Kan^R *usp-2* mutants (ecotype Columbia) contained a large proportion of collapsed pollen grains compared to pollen from wild-type flowers (data not shown). A significant difference in flowering time between wild type and heterozygotes from either *usp-1* or *usp-2* lines was not observed under a 24 h light regime (data not shown).

To determine if the collapsed pollen grains were viable, we used Alexander's viability stain (Alexander 1969). In this staining procedure, the cellulose in the pollen wall produces a green color, and the protoplasm produces a purple color (Alexander 1980). All four pollen grains in tetrads from L12WT were viable (Fig. 2c). In contrast, the two collapsed grains of the tetrad from *usp-1* heterozygous plants were nonviable (Fig. 2d). Collapsed pollen isolated from the heterozygous *usp-2* mutants was also nonviable (data not shown).

We stained mature pollen with 4′,6-diamidino-2-phenylindole (DAPI) to visualize the nuclear phenotype. Tetrads from L12WT contained four pollen grains, each with a vegetative nucleus and two smaller sperm nuclei (Fig. 2e, g). In pollen tetrads from L9HET, only the two wild-type pollen grains showed nuclear staining (Fig. 2f, h). The lack of DAPI staining in collapsed *usp-1* pollen grains indicated the absence of nuclei at pollen maturity.

To confirm that collapsed pollen in tetrads of L9HET were nonviable, we tested pollen germination. Pollen collected from flowers of both wild-type and heterozygous *usp-1* plants was incubated on pollen germination medium. In pollen from L12WT, 604 tetrads showed germination. Of these, 559 had one or two germinated pollen grains of the tetrad, and 45 tetrads contained three or four germinated pollen grains. In contrast, none ($n = 707$) of the germinated pollen tetrads in the L9HET line had three or four germinated pollen grains of the tetrad.

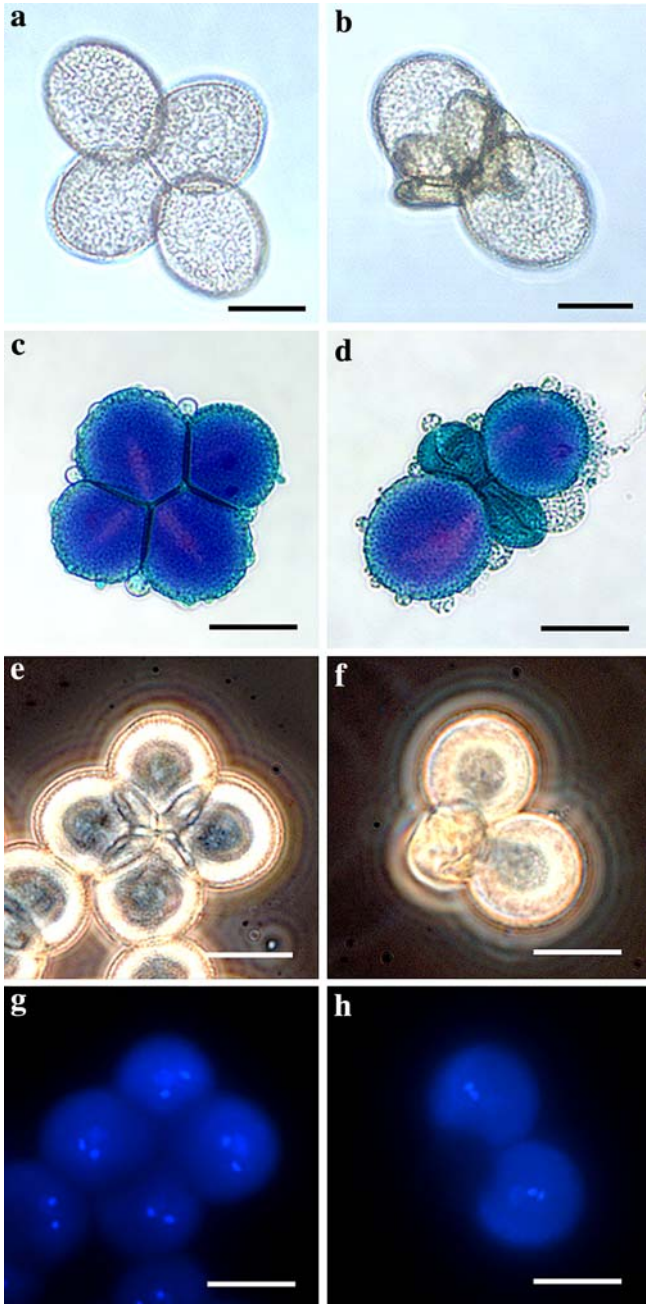

Fig. 2 Phenotype of pollen isolated from wild-type and heterozygous *usp-1* plants. **a** Pollen tetrad from L12WT line. **b** Pollen tetrad from a heterozygous *usp-1* line. Alexander's stain for viability in a pollen tetrad from L12WT (**c**) and L9HET *usp-1* mutant (**d**). DAPI staining of pollen tetrads from L12WT (**e**, **g**) and L9HET (**f**, **h**). Images are shown as bright field (**e**, **f**) and DAPI fluorescence (**g**, **h**). Scale bars represent 20 μm

a

# of viable pollen grains per tetrad

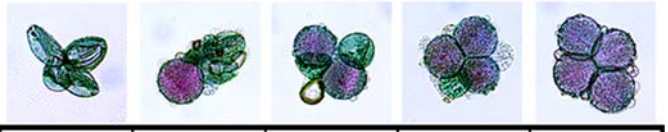

Line	0	1	2	3	4
L12WT	3	0	2	6	269
L9HET	5	6	265	0	0
L10-1C	8	6	6	22	156
L10-5C	5	7	49	46	48

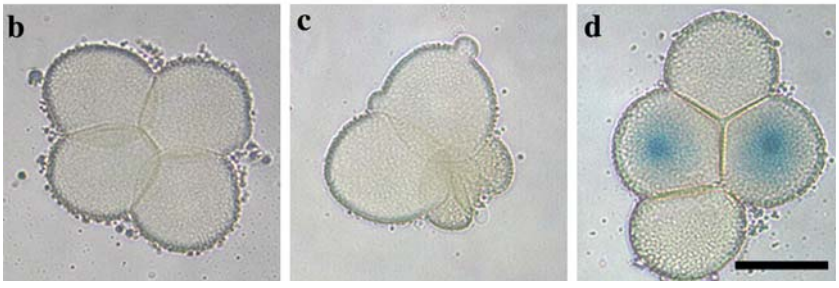

Fig. 3 Complementation of the pollen phenotype in *usp-1* mutants transformed with a *AtUSP*prom:*AtUSP*cDNA construct. **a** Alexander's viability stain in pollen tetrads of L12WT, L9HET, and two complemented lines (L10-1C and L10-5C). **b-d** Histochemical GUS staining of pollen from L12WT (**b**), L9HET (**c**), and L10-1C (**d**). Scale bars represent 20 μm

Complementation of *usp-1*

To determine if the collapsed pollen phenotype in heterozygous *usp* mutants was caused by the presence of a mutant *usp* allele, we created a transformation construct containing *NPTII* and the *AtUSP* cDNA under control of the native *AtUSP* promoter. Basta-resistant *usp-1* plants (L10H; 15 of 28 T_2 Ba^R) were transformed and genomic DNA from plants resistant to both kanamycin and Basta was screened by PCR. Two individuals, L10-1C and L10-5C, yielded PCR fragments corresponding to the presence of a wild-type *AtUSP* allele, *usp-1*, and *NPTII* DNA fragments (data not shown).

We used Alexander's stain to quantify pollen viability in the complemented lines. As shown in Fig. 3a, 98% of tetrads in line L12WT contained three or four viable pollen grains. In pollen from line L9HET, 98% of tetrads contained only one or two viable pollen grains and the remaining 2% of tetrads had no viable pollen grains. In pollen from line L10-1C and L10-5C, 90% and 61% of tetrads contained three or four viable pollen grains, respectively (Fig. 3a). Complementation of the phenotype was further confirmed by histochemical staining pollen for GUS activity. The T-DNA used to generate the *usp-1* line contains the *β*-glucuronidase (GUS) gene driven by the pollen-specific *LAT52* promoter (Sessions et al. 2002). As expected, no staining was observed when tetrads from L12WT were stained for GUS activity (Fig. 3b). No visible staining was observed in tetrads from L9HET (Fig. 3c), probably due to the lack of nuclear material in the collapsed grains (Fig. 2h). However, in tetrads from L10-1C and L10-5C, GUS staining was observed in pollen grains restored to wild-type appearance (Fig. 3d). Pollen tetrads with three or four germinating pollen grains were observed in these lines, showing restoration of viability (data not shown).

Characterization of the pollen phenotype

To determine the nature of the defect in *usp* pollen, we used electron microscopy (EM) to visualize surface and ultrastructural characteristics. To analyze the surface, pollen from *usp-1* and *usp-2* flowers was collected and coated with gold particles for visualization by scanning EM. The characteristic reticulate patterning of the exine was present in pollen from L12WT (Fig. 4a, b) and L9HET (Fig. 4c, d), but appeared compressed in the collapsed grains. In *usp-2*, collapsed pollen grains were present and exine was similar in appearance to wild-type pollen (Fig. 4e).

To determine whether ultrastructural differences existed within mutant pollen grains, we prepared samples for transmission EM (TEM). For these studies, we chose to use the mutant line in the Columbia background (*usp-2*) to minimize confusion in deciphering pollen structure within fused grains of the *quartet* background (*usp-1*). In stage 12 anthers (staged according to Sanders et al. 1999) from *usp-2* flowers, pollen grains were mature. Fig. 5 shows both a wild-type (a) and *usp-2* mutant pollen grain (b). At this stage, prior to dehiscence, mutant pollen appeared collapsed and little or no cytoplasmic contents were evident. The exine in the collapsed pollen appeared to be intact, as seen in SEM images (Fig. 4).

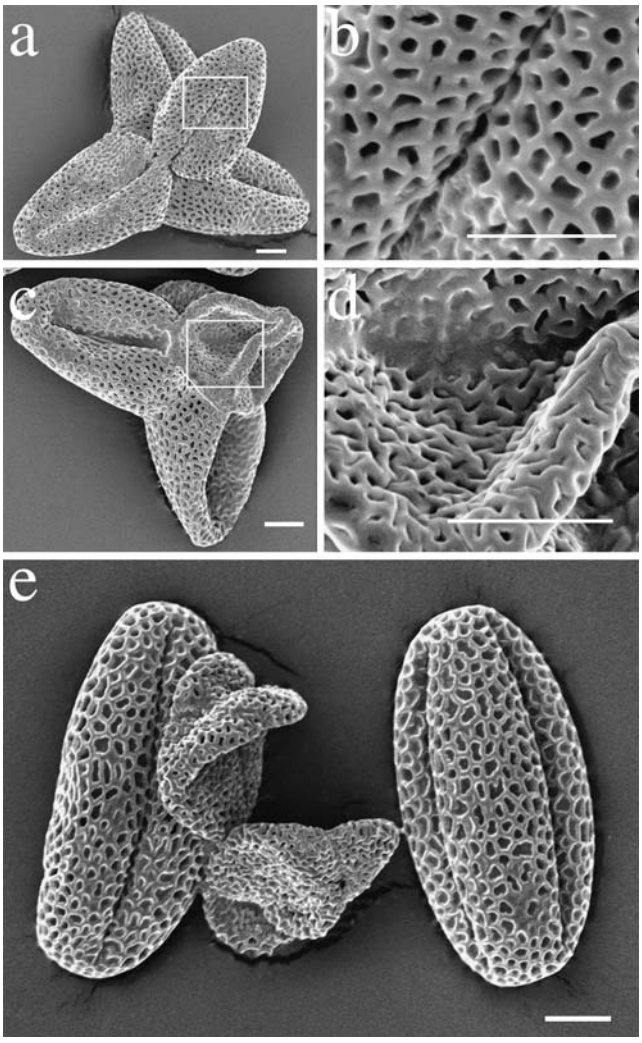

Fig. 4 SEM of pollen isolated from wild-type and heterozygous plants (*usp-1*) and heterozygous *usp-2* plants. **a** A pollen tetrad from L12WT. Higher magnification of the boxed area to show detail is shown (**b**). **c** Pollen tetrad from a heterozygous *usp-1* flower. Higher magnification of the boxed area to show detail is shown (**d**). **e** Pollen grains isolated from a heterozygous *usp-2* plant. Scale bars represent 5 μm

At an earlier stage of anther development (stage 11), differentiation between wild-type and mutant pollen grains was again straightforward (Fig. 6a, b). Some mutant pollen grains were beginning to show signs of collapse while the wild-type pollen remained turgid. The majority of mutant pollen grains were similar to wild type in size yet had severely degraded cytoplasm. At higher magnification, it was evident that intine was present in wild-type pollen (Fig. 6c, e) but absent in mutant pollen (Fig. 6d, f).

Wild-type pollen grains at stage 9 of anther development have a less-developed exine structure and intine appears to be in the process of deposition (Fig. 7). At this stage, it was still possible to phenotype most of the pollen grains. As shown in Fig. 7a, the pollen grains with darkly staining cytoplasm were wild-type and accordingly showed the presence of an intine layer (Fig. 7b). Most pollen grains lacking any discernable intine (Fig. 7c) contained degraded cytoplasm, as seen in stage 11 mutant pollen grains. A proportion of pollen grains were difficult to phenotype, as the shade of cytoplasmic staining was intermediate and the presence of an intine (albeit thinner) could not be ruled out (Fig. 7d).

Cell wall analysis in *usp-1*

The lack of transmission of *usp* through the male gametophyte prevented the development of homozygous plants. Throughout growth and development, the heterozygous *usp-1* and *usp-2* plants were indistinguishable from wild-type plants under standard growing conditions. Although heterozygous plants did not exhibit an obvious visible phenotype, we examined whether the mutation caused chemical changes in cell wall composition. AtUSP has been shown to synthesize UDP-GlcA, a precursor of cell wall constituents (L.A. Litterer et al., submitted). In heterozygous *usp* plants, the reduced level of *AtUSP* transcript (Fig. 1b) could potentially change cell wall composition. T_2 seed from the heterozygous line L9HET was used, and at 42 days, plants were flowering and the phenotype of the pollen could be determined to differentiate wild-type from heterozygous lines. Dried rosette and stem samples were pulverized for cell wall analysis and the results are summarized in Table 2. The amount of cell wall material was measured as the sum of Klason lignin, Glc, Xyl, Man, Fuc, UA, Ara, Gal, and Rha. For all cell wall components tested, no significant differences ($P > 0.05$) between wild-type and heterozygous lines were observed within the same tissue type (Table 2).

Determination of USP activity

To determine if a phenotype was present at a biochemical level, we assayed rosette tissues for USP (UDP-GlcA → GlcA-1-P) activity. Plants from a segregating population of *usp-1* (L9HET) were phenotyped by scoring pollen from newly bolted plants. Inflorescences were discarded and rosettes corresponding to wild-type or heterozygotes were ground and extracted. Desalted crude extracts were incubated with ^{14}C-UDP-GlcA and the conversion to labeled GlcA-1-P was quantified. Rosettes of the heterozygous plants averaged 50.2% lower USP activity than that of wild type (Fig. 8). This result suggests that AtUSP may be responsible for a large proportion of USP activity (UDP-GlcA → GlcA-1-P) in vivo.

Discussion

The data presented here show that AtUSP is essential for the development of viable pollen. Evaluation of two

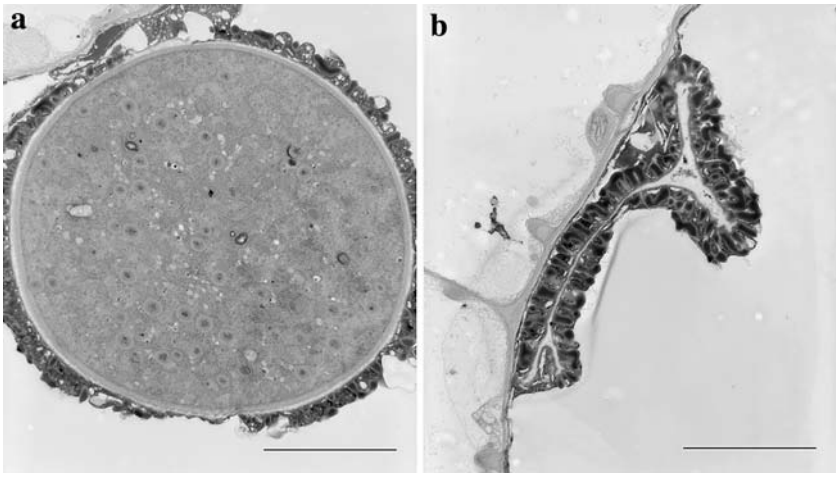

Fig. 5 TEM within a stage 12 anther of a heterozygous *usp-2* flower showing a wild-type pollen grain (**a**) and a collapsed mutant pollen grain (**b**). Scale bars represent 10 μm

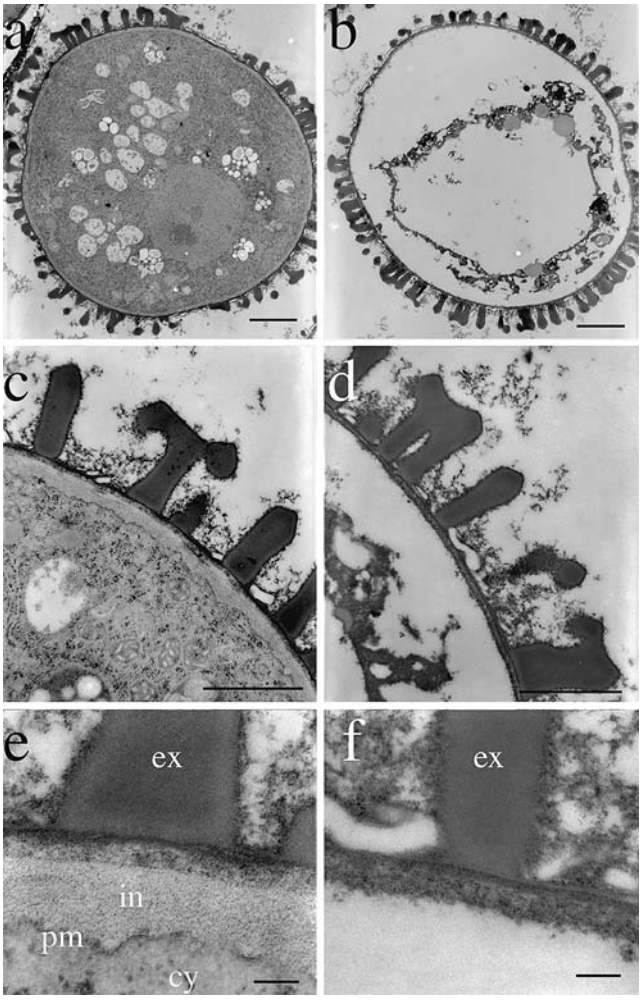

Fig. 6 TEM of pollen grains within a stage 11 anther of a heterozygous *usp-2* flower. Wild-type pollen (**a**, **c**, **e**) and *usp-2* mutant pollen (**b**, **d**, **f**) contained intact exine but pollen of *usp-2* lacked discernable intine. Scale bars represent 2 μm (**a**, **b**), 1 μm (**c**, **d**), and 0.1 μm (**e**, **f**). *Ex* exine, *in* intine, *pm* plasma membrane, *cy* cytoplasm

independent T-DNA insertional alleles showed that disruption of *AtUSP* results in collapsed pollen grains that lack an inner wall, the intine (Figs. 5, 6, 7). Further evidence showing that the collapsed pollen phenotype was due to the mutant *usp* allele was shown by complementation with the *AtUSP* cDNA (Fig. 3). Genetic analysis by reciprocal test crosses indicated that insertional mutagenesis of *AtUSP* had no effect on the female gametophyte (Table 1).

USP is a novel broad substrate pyrophosphorylase that appears to be unique to plants (L.A. Litterer et al., submitted), but its function has not been clearly defined. Two functions for USP have been proposed. One function involves salvage of monosaccharides formed by hydrolysis of glycoconjugates and polysaccharides during metabolism (Kotake et al. 2004). This function would involve turnover and recycling of monosaccharides released during hydrolytic reactions in the cytosol, as well as recycling monosaccharides such as Gal and Ara formed in the cell wall during synthesis and modification (Gibeaut and Carpita 1991; Lozovaya et al. 1996; Gorshkova et al. 1997). The second proposed function for AtUSP involves serving as UDP-GlcA pyrophosphorylase (EC 2.7.7.44), the terminal enzyme of MIO pathway (L.A. Litterer et al., submitted). In this role, USP could contribute to the synthesis of UDP-GlcA, a key precursor for the synthesis of cell wall matrix polysaccharides. The gene for UDP-GlcA pyrophosphorylase has not been identified, but the relatively high activity and affinity of AtUSP for GlcA-1-P measured in vitro suggests that it could serve as the terminal enzyme of the MIO pathway (L.A. Litterer et al., submitted). Both proposed functions of USP could impact cell wall formation in plants. Hence, it is possible that lack of intine observed in *usp* pollen is due to one or both of the proposed functions. Intine synthesis is initiated during the early stages of male gametogenesis and is controlled by the male gametophyte (Taylor et al. 1998; Ariizumi et al. 2004). This is in contrast to the exine, the outer pollen wall that is composed primarily of sporopollenin. Sporopollenin, a biopolymer formed

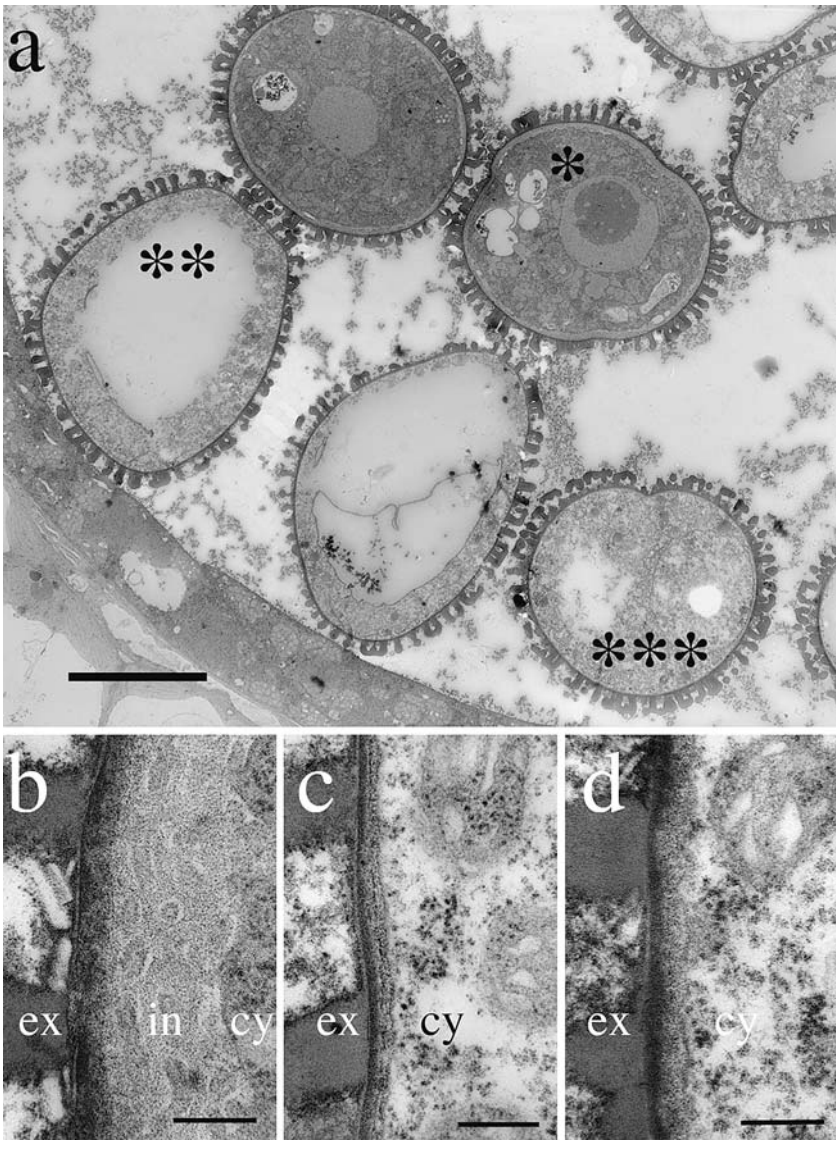

Fig. 7 TEM of *usp-2* pollen grains at anther stage 9. **a** Overview of five pollen grains. **b** Higher magnification of the wall in the pollen grain (**a**) marked with (*asterisks*). **c** Higher magnification of the wall in the pollen grain (**a**) marked with (*double asterisks*). **d** Higher magnification of the wall in the pollen grain (**a**) marked with (*triple asterisks*). Scale bars represent 10 μm (**a**), and 0.25 μm (**b–d**). *Ex* exine, *in* intine, *cy* cytoplasm

Table 2 Cell wall composition of rosettes and stems of wild-type (*qrt1*/*qrt1*;*USP*/*USP*) and mutant (*qrt1*/*qrt1*;*USP*/*usp-1*) plants at 42 days

Plant	Tissue	CW g/kg OM	KL mg/g CW	Glc mg/g CW	Xyl mg/g CW	Man mg/g CW	Fuc mg/g CW	UA mg/g CW	Ara mg/g CW	Gal mg/g CW	Rha mg/g CW
USP/*USP*	Rosette	315	217	247	56	33	7.7	321	40	57	23
USP/*usp-1*	Rosette	316	214	252	56	33	7.3	316	41	57	24
USP/*USP*	Stem	598	221	393	145	30	1.3	151	20	27	11
USP/*usp-1*	Stem	613	239	383	145	30	1.3	146	19	26	11
SEM	—	14	8	3	2	1	0.3	6	1	1	1

Significant differences between tissue types (rosette vs. stem) were found, but differences observed between the same tissue type of wild type and mutant were not statistically significant ($P > 0.05$)
CW cell wall, *OM* organic matter, *KL* Klason lignin, *Glc* glucose, *Xyl* xylose, *Man* mannose, *Fuc* fucose, *UA* uronic acids, *Ara* arabinose, *Gal* galactose, *Rha* rhamnose, *SEM* standard error of the mean

from lipid and phenylpropanoid precursors, is synthesized by the sporophytic tapetum (Scott et al. 2004). The presence of a mutant *usp* allele had little or no visible effect on exine formation.

It is not obvious how the loss of the proposed salvage function of AtUSP would prevent intine formation. Although the salvage pathway for nucleotide sugar synthesis has been known to exist in plants for over

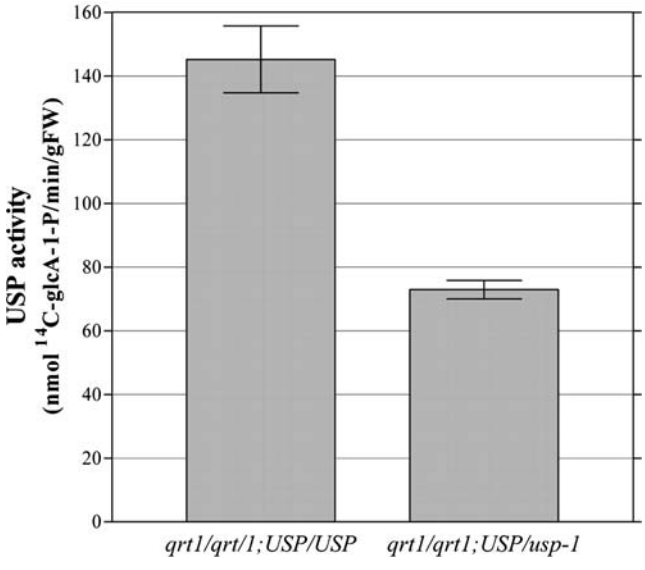

Fig. 8 Comparison of USP (UDP-GlcA → GlcA-1-P) activity in wild-type and heterozygous *usp-1* rosettes. Values are means ± SE ($n = 6$)

25 years, its relative importance in plant metabolism has not been clearly defined (Feingold and Avigad 1980). It cannot be ruled out that the salvage pathway plays a key, but yet undefined role in the early stages of male gametogenesis, and that degradation of cytoplasm and lack of intine are indirect consequences of the mutation.

A critical function of AtUSP in pollen development may be its proposed role as the terminal enzyme of the MIO pathway (L.A. Litterer et al., submitted). It is more apparent that blocking this function could interfere with intine formation. The MIO pathway produces UDP-GlcA, a key precusor for the synthesis of cell wall matrix polysaccharides. The formation of the pectocellulosic intine may require synthesis of matrix polysaccharides via the MIO pathway. If the synthesis of matrix polysaccharides is blocked, cellulose synthesis may also be impaired. Inhibition of intine synthesis during the early stages of male gametogenesis may arrest pollen development leading to collapsed, aborted pollen.

The hypothesis that the lethal effect of *usp* in pollen is due to blockage of the MIO pathway is based on the assumption that UDP-GlcA biosynthesis in developing pollen is dependent upon this pathway. However, the nucleotide sugar oxidation (NSO) pathway, an alternate pathway for the production of UPD-GlcA, exists in plants (Feingold and Avigad 1980; Kärkönen 2005). The NSO pathway, involving the conversion of UDP-Glc to UDP-GlcA is catalyzed by UDP-Glc dehydrogenase. The relative contributions of the two pathways to UDP-GlcA biosynthesis have not been evaluated in developing pollen, but research has indicated that the relative importance of the two pathways for UDP-GlcA synthesis in various plant tissues is dependent on tissue and stage of development (Seitz et al. 2000; Kärkönen 2005). It is possible that the NSO pathway is not operational in developing pollen.

In contrast to the effects of a mutant *usp* allele on the male gametophyte, the female gametophyte was unaffected (Table 1). The results indicated that AtUSP is not required for megaspore formation or development of the embryo sac. It is possible that the two proposed functions for USP described above are not critical during female gametogenesis. Alternatively, the NSO pathway may predominate in tissues of the embryo sac and the absence of a functional MIO pathway would therefore have no impact on viability.

Because *usp* was not transmitted through pollen, homozygous plants could not be obtained for analysis. In sporophytic tissues of heterozygous plants, *AtUSP* transcript was reduced (Fig. 1b) but no obvious phenotype was apparent under standard growing conditions. Associated with a reduction of *AtUSP* transcript in the heterozygous plants was a reduction in USP activity, as measured with UDP-GlcA as substrate (Fig. 8). This result suggests that AtUSP may be responsible for the majority of UDP-GlcA pyrophosphorylase activity in Arabidopsis. In earlier studies conducted with semi-purified fractions, it was generally assumed that UDP-GlcA pyrophosphorylase activity measured was that of the terminal enzyme of the MIO pathway (Roberts 1971; Roberts and Cetorelli 1973; Dickinson et al. 1977; Feingold and Avigad 1980; Hondo et al. 1983). However, the substrate specificity of purified UDP-GlcA pyrophosphorylase was never determined. Our results suggest that AtUSP, a broad substrate pyrophosphorylase, may be responsible for most of the UDP-GlcA pyrophosphorylase activity measured in Arabidopsis rosettes. Further research involving the use of a monoclonal antibodies for AtUSP will be required to determine if UDP-GlcA pyrophophorylase activity measured in plants is solely due to the gene product of *AtUSP*.

The presence of a mutant *usp* allele resulted in the lack of pectocellulosic intine in developing pollen, yet had no effect on cell wall composition in vegetative heterozygous tissues. Assuming the gene product of AtUSP acts as the terminal enzyme of the MIO pathway, the interpretation of this finding is not simple. One interpretation is that the NSO pathway is the dominant pathway for the synthesis of cell wall matrix polysaccharides in sporophytic tissues. Alternatively, the MIO pathway may play an important role in the synthesis of UDP-GlcA, but under normal growth conditions, a 50% reduction in enzyme activity does not impair its function as terminal enzyme in the MIO pathway. Future research using RNAi technology will be needed to determine whether greater than a 50% reduction in *AtUSP* transcript produces a phenotype in the sporophyte.

A recent report examined the effect of insertional mutagenesis of UDP-Glc dehydrogenase (*UGD*) in maize (Kärkönen et al. 2005). *UGD* encodes the enzyme that catalyzes the formation of UDP-GlcA via the NSO pathway. Two putative *UGD* genes were identified in maize. A homozygous knockout of one of the *UGD*

genes (*udpgdh-A1*) reduced UGD enzyme activity in developing maize leaves by approximately 90%. The knockout did not result in an obvious phenotype nor did it change cell wall cellulose content. However, cell wall pentose content was reduced based on measurements of Ara/Gal and Xyl/Gal ratios in the alcohol insoluble residue from maize leaves. Kärkönen et al. (2005) concluded that in maize leaf tissue, the NSO pathway was probably of greater importance than the MIO pathway for the synthesis of UDP-GlcA.

Several mutations that affect pollen wall development and result in male sterility have been reported in Arabidopsis. The *dex1*, *nef1*, *flp1* and *ms2* mutations result in a defective exine (Aarts et al. 1997; Paxson-Sowders et al. 1997, 2001; Ariizumi et al. 2003, 2004;). Evidence suggests that these mutations result in inhibition of the deposition or synthesis of sporopollenin, the biopolymer from which the exine is formed. Two Arabidopsis pollen mutations that impair intine formation, *ms8* and *mad3*, have been reported (Taylor et al. 1998; Grini et al. 1999). Both mutations can produce collapsed, aborted pollen. The *ms8* mutation is a sporophytic lesion that may affect the tapetum (Taylor et al. 1998). The basis for the *mad3* mutation has not been identified (Grini et al. 1999).

Although our results clearly show that disruption of *AtUSP* blocks normal male gametogenesis, the specific cause of the collapsed pollen phenotype lacking an intine has not been defined. One explanation for the collapsed pollen phenotype, based on the functions of USP proposed to date, is that the absence of a functional *AtUSP* allele interferes with the MIO pathway. This in turn could block the synthesis of matrix polysaccharides which are required for intine synthesis during the early stages of male gametophytic development. Inhibiting intine synthesis may arrest pollen development and eventually result in shrunken, aborted pollen. This hypothesis assumes that the NSO pathway is not operational in developing pollen and hence cannot compensate for the inhibition of the MIO pathway. It is also possible that a critical function of *AtUSP*, not yet identified, may be responsible for the lethal effect of the mutation in developing pollen.

Acknowledgements The authors are grateful to Gib Ahlstrand for assistance with scanning and transmission electron microscopy and Ted Jeo for cell wall carbohydrate analysis. We would also like to thank Renee Schirmer and Ann Chaptman for technical assistance.

References

Aarts MG, Hodge R, Kalantidis K, Florack D, Wilson ZA, Mulligan BJ, Stiekema WJ, Scott R, Pereira A (1997) The Arabidopsis MALE STERILITY 2 protein shares similarity with reductases in elongation/condensation complexes. Plant J 12:615–623

Ahmed AER, Labavitch JM (1977) A simplified method for accurate determination of cell wall uronide content. J Food Biochem 1:361–365

Alexander MP (1980) A versatile stain for pollen, fungi, yeast and bacteria. Stain Technol 55:13–18

Alexander MP (1969) Differential staining of aborted and non-aborted pollen. Stain Technol 44:117–122

Alonso JM, Stepanova AN, Leisse TJ, Kim CJ, Chen H, Shinn P, Stevenson DK, Zimmerman J, Barajas P, Cheuk R, Gadrinab C, Heller C, Jeske A, Koesema E, Meyers CC, Parker H, Prednis L, Ansari Y, Choy N, Deen H, Geralt M, Hazari N, Hom E, Karnes M, Mulholland C, Ndubaku R, Schmidt I, Guzman P, Aguilar-Henonin L, Schmid M, Weigel D, Carter DE, Marchand T, Risseeuw E, Brogden D, Zeko A, Crosby WL, Berry CC, Ecker JR (2003) Genome-wide insertional mutagenesis of *Arabidopsis thaliana*. Science 301:653–657

Ariizumi T, Hatakeyama K, Hinata K, Inatsugi R, Nishida I, Sato S, Kato T, Tabata S, Toriyama K (2004) Disruption of the novel plant protein NEF1 affects lipid accumulation in the plastids of the tapetum and exine formation of pollen, resulting in male sterility in *Arabidopsis thaliana*. Plant J 39:170–181

Ariizumi T, Hatakeyama K, Hinata K, Sato S, Kato T, Tabata S, Toriyama K (2003) A novel male-sterile mutant of *Arabidopsis thaliana*, faceless pollen-1, produces pollen with a smooth surface and an acetolysis-sensitive exine. Plant Mol Biol 53:107–116

Clough SJ, Bent AF (1998) Floral dip: a simplified method for Agrobacterium-mediated transformation of *Arabidopsis thaliana*. Plant J 16:735–743

Dickinson DB, Hyman D, Gonzales JW (1977) Isolation of uridine 5′-pyrophosphate glucuronic acid pyrophosphorylase and its assay using ^{32}P-pyrophosphate. Plant Physiol 59:1082–1084

Feingold DS, Avigad G (1980) Sugar nucleotide transformations in plants. In: Stumpf PK, Conn EE (eds) The biochemistry of plants: a comprehensive treatise, vol 3. Academic, New York, pp 101–170

Feingold DS, Neufeld EF, Hassid WZ (1958) Enzymic synthesis of uridine diphosphate glucuronic acid and uridine diphosphate galacturonic acid with extracts from *Phaseolus aureus* seedlings. Arch Biochem Biophys 78:401–406

Gibeaut DM, Carpita NC (1991) Tracing cell wall biogenesis in intact cells and plants: Selective turnover and alteration of soluble and cell wall polysaccharides in grasses. Plant Physiol 97:551–561

Giberson RT, Demaree RE Jr Nordhausen RW (1997) Four-hour processing of clinical/diagnostic specimens for electron microscopy using microwave technique. J Vet Diagn Invest 9:61–67

Gorshkova TA, Chemikosova SB, Lozovaya VV, Carpita NC (1997) Turnover of galactans and other cell wall polysaccharides during development of flax plants. Plant Physiol 114:723–729

Grini PE, Schnittger A, Schwarz H, Zimmermann I, Schwab B, Jürgens G, Hülskamp M (1999) Isolation of ethyl methanesulfonate-induced gametophytic mutants in *Arabidopsis thaliana* by a segregation distortion assay using the multimarker chromosome 1. Genetics 151:849–863

Hanaichi T, Sato T, Iwamoto T, Malavasi-Yamashiro J, Hoshino M, Mizuno N (1986) A stable lead by modification of Sato's method. J Electron Microsc 35:304–306

Hondo T, Hara A, Funaguma T (1983) Purification and properties of UDP-glucuronate pyrophosphorylase from pollen of *Typha latifolia* Linne. Plant Cell Physiol 24:1535–1543

Howden R, Park SK, Moore JM, Orme J, Grossniklaus U, Twell D (1998) Selection of T-DNA-tagged male and female gametophytic mutants by segregation distortion in Arabidopsis. Genetics 149:621–631

Jefferson RA, Kavanagh TA, Bevan MW (1987) GUS fusions: beta-glucuronidase as a sensitive and versatile gene fusion marker in higher plants. EMBO J 6:3901–3907

Johnson-Brousseau SA, McCormick S (2004) A compendium of methods useful for characterizing Arabidopsis pollen mutants and gametophytically-expressed genes. Plant J 39:761–775

Kärkönen A (2005) Biosynthesis of UDP-GlcA: via UDPGDH or the *myo*-inositol oxidation pathway? Plant Biosystems 139:46–49

Kärkönen A, Murigneux A, Martinant J-P, Pepey E, Tatout C, Dudley BJ, Fry SC (2005) UDP-glucose dehydrogenases of

maize: a role in cell wall pentose biosynthesis. Biochem J 391:409–415

Kotake T, Yamaguchi D, Ohzono H, Hojo S, Kaneko S, Ishida HK, Tsumuraya Y (2004) UDP-sugar pyrophosphorylase with broad substrate specificity toward various monosaccharide 1-phosphates from pea sprouts. J Biol Chem 279:45728–45736

Klimyuk VI, Carroll BJ, Thomas CM, Jones JD (1993) Alkali treatment for rapid preparation of plant material for reliable PCR analysis. Plant J 3:493–494

Loewus FA, Loewus MW (1983) *myo*-Inositol: Its biosynthesis and metabolism. Ann Rev Plant Physiol 34:137–161

Lozovaya VV, Zabotina OA, Widholm JM (1996) Synthesis and turnover of cell-wall polysaccharides and starch in photosynthetic soybean suspension cultures. Plant Physiol 111:921–929

Otozai K, Taniguchi H, Nakamura M (1973) UDP-glucose pyrophosphorylase from tubers of Jerusalem artichoke (*Helianthus tuberosus* L.). Agr Biol Chem 37:531–537

Paxson-Sowders DM, Dodrill CH, Owen HA, Makaroff CA (2001) DEX1, a novel plant protein, is required for exine pattern formation during pollen development in Arabidopsis. Plant Physiol 127:1739–1749

Paxson-Sowders DM, Owen HA, Makaroff CA (1997) A comparative ultrastructural analysis of exine pattern development in wild-type *Arabidopsis* and a mutant defective in pattern formation. Protoplasma 198:53–65

Preuss D, Rhee SY, Davis RW (1994) Tetrad analysis possible in Arabidopsis with mutation of the QUARTET (QRT) genes. Science 264:1458–1460

Roberts RM (1971) The formation of uridine diphosphate-glucuronic acid in plants: uridine diphosphate-glucuronic acid pyrophosphorylase from barley seedlings. J Biol Chem 246:4995–5002

Roberts RM, Cetorelli JJ (1973) UDP-D-Glucuronic acid pyrophosphorylase and the formation of UDP-D-glucuronic acid in plants. In: Loewus F (ed) Biogenesis of plant cell wall polysaccharides. Academic, New York, pp 49–68

Sanders PM, Bui AQ, Weterings K, McIntire KN, Hsu YC, Lee PY, Truong MT, Beals TP, Goldberg RB (1999) Anther developmental defects in *Arabidopsis thaliana* male-sterile mutants. Sex Plant Reprod 11:297–322

Seitz B, Klos C, Wurm M, Tenhaken R (2000) Matrix polysaccharide precursors in Arabidiopsis cell walls are synthesized by alternate pathways with organ-specific expression patterns. Plant J 21:537–546

Schnurr J, Shockey J, Browse J (2004) The acyl-CoA synthetase encoded by LACS2 is essential for normal cuticle development in Arabidopsis. Plant Cell 16:629–642

Scott RJ, Spielman M, Dickinson HG (2004) Stamen structure and function. Plant Cell 16:S46–S60

Sessions A, Burke E, Presting G, Aux G, McElver J, Patton D, Dietrich B, Ho P, Bacwaden J, Ko C, Clarke JD, Cotton D, Bullis D, Snell J, Miguel T, Hutchinson D, Kimmerly B, Mitzel T, Katagiri F, Glazebrook J, Law M, Goff SA (2002) A high-throughput Arabidopsis reverse genetics system. Plant Cell 14:2985–2994

Sowokinos JR, Spychalla JP, Desborough SL (1993) Pyrophosphorylases in *Solanum tuberosum* IV. Purification, tissue localization, and physiochemical properties of UDP-glucose pyrophosphorylase. Plant Physiol 101:1073–1080

Szumilo T, Zeng Y, Pastuszak I, Drake R, Szumilo H, Elbein AD(1996) Purification to homogeneity and properties of UDP-GlcNAc (GalNAc) pyrophosphorylase. J Biol Chem 271:13147–13154

Taylor PE, Glover JA, Lavithis M, Craig S, Singh MB, Knox RB, Dennis ES, Chaudhury AM (1998) Genetic control of male fertility in *Arabidopsis thaliana*: structural analyses of postmeiotic developmental mutants. Planta 205:492–505

Theander O, Aman P, Westerlund E, Andersson R, Pettersson D (1995) Total dietary fiber determined as neutral sugar residues, uronic acid residues, and Klason lignin (The Uppsala Method): collaborative study. J AOAC Int 78:1030–1044